Nonlinear Control of a Novel DC Linear Motor

Ugur Hasirci, and Ziya Demirkol

***Abstract*—This study concerns the design and simulation of a nonlinear controller for a novel Direct Current (DC) Linear Induction Motor. The motor offers a very high force/current ratio and this makes it ideal for many applications. Controlling the motor current, position and speed is one of the key requirements for operational processes in this applications. The controller introduced in this study aims to track a desired velocity profile by assuming all the system parameters are exactly known, that it, it is an exact model knowledge controller. The paper first explains the development of the dynamical model of the system, then the design of the controller step-by-step, and finally it provides the numerical simulation results of the designed controller. Lyapunov-type arguments have been used for stability analysis of the designed controller.**

***Keywords*—DC linear motors, Nonlinear control, Lyapunov Stability Theory, Numerical simulation.**

I. Introduction

Electric motors are one of the primary components in the industry to produce torque or force by converting electrical energy into mechanical energy. Even if they may be classified in many ways, the most general classification is direct current (DC), alternating current (AC) and synchronous motor. Each type has certain advantages and disadvantages and the process determines the best option. A DC motor offers some advantages like easier speed regulation as well as some disadvantages like higher fault risk and maintenance requirement compared to an AC counterpart.

A classical DC motor produces rotary motion. But if a linear movement is needed in any industrial processes, the DC machine designer has two options; either a rotary DC motor is used by using some additional apparatus to convert rotary motion into linear motion, or a linear DC motor can be used. The former has some disadvantages like additional losses and costs introduced by conversion systems. But the main problem with the use of linear DC motor is due to their low force/current ratio and short stroke distance. In fact, many designs for the linear DC motor have been presented in the literature but most of them suffer from low force/current ratio. For example, for 1 A current, the developed force is 2.67 N in [1], 27 N in [2], 1 N in [3], 7.8 N in [4], 1 N [5], and 24 N in [6]. A very recent study [7] reports generation of 27 N force per ampere. Reported experimental results clearly show that there is still a need to improve force/current ratio for this type of motor to be able use them for some special applications like electromagnetic launchers. A novel design for this type of motors has been offered recently to get higher force/current ratio. Its design, implementation and test are given in [8], some additional experimental results are given in [9]. This patented [10] design produces 200 N/A force/current ratio. Its sketch is given in Fig. 1. An implemented form of the design is given in Fig. 2.

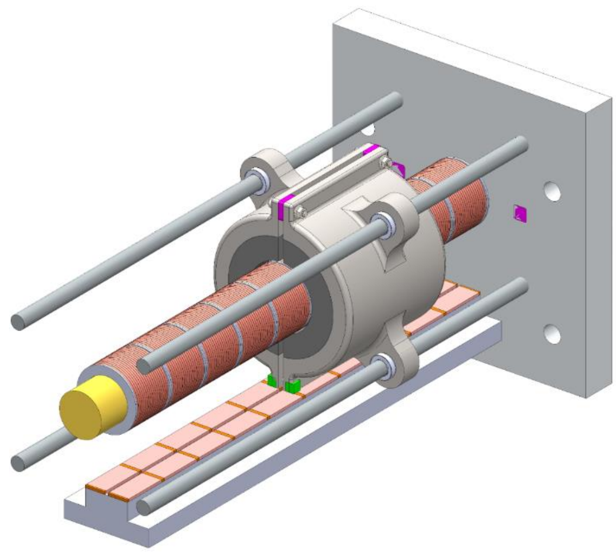

Fig. 1. A 3D sketch of a novel permanent magnet DC linear motor

Fig. 2. Test setup

Control of this new motor is an important aspect to be able to use it in some industrial processes. A controller for this type of motor has been presented in [11] but this controller is linear controller and assumes the motor operates in no-load condition, i.e., the load force is equal to zero. In this study, on the other hand, it is assumed that the motor operates with a load and the load dynamics are nonlinear.

Manuscript received May 19, 2025. This work was supported in part by the Scientific and Technological Research Council of Turkiye (TUBITAK) under Grant 124E435.

U. Hasirci is with the Duzce University, Duzce, 81620 Turkiye
Z. Demirkol is with Kastamonu University, Kastamonu, 37100 Turkiye.

This paper concerns the design and simulation of a nonlinear controller for the novel DC linear motor introduced above. It is assumed that all the system parameters are exactly known. During the controller design, Lyapunov-type arguments have been used the stability of the system as well as the boundedness of all the signals in the closed-loop system. To show the performance and feasibility of the controller, a numerical simulation by using MATLAB/Simulink [12] environment has been also provided.

The rest of the paper is organized as follows. Section II develops a dynamical model of the system to be controlled. Section III defines the control problem. Design of the nonlinear controller is explained in Section IV. Numerical simulation results are given in Section V. The last section concludes some remarks also with some future consideration.

II. Dynamical Model Derivation

Mechanical part of the dynamical model of a Permanent Magnet DC Linear Motor can simply be derived by using the Second Law of Newton as

$$\Sigma F(t) = ma(t) \tag{1}$$

where $F(t)$ is the total force acting on the moving part, m reprensents the mass of the moving part, and $a(t)$ depicts the acceleration of the moving part. Eq. (1) can be also expressed as

$$F_e(t) - F_s(t) - F_L(t) = m\frac{d^2x(t)}{dt^2} \tag{2}$$

where $F_e(t)$ is the developed electrical force, $F_s(t)$ stands for the friction force acting on the moving part, $F_L(t)$ is the load force, and $x(t)$ is the position of the moving part. In this study, the friction force will be assumed as

$$F_s(t) = \alpha\frac{dx(t)}{dt} \tag{3}$$

where α is the viscous friction coefficient, the load force will be assumed to be nonlinear as

$$F_L(t) = \beta\sin x(t) \tag{4}$$

where β is the load coefficient, and the developed electrical force acting on the moving part, $F_e(t)$, is expressed as

$$F_e(t) = Ki_a(t) \tag{5}$$

where K is the force constant of the machine, and $i_a(t)$ is the armature current. In this way, the differential equation model of the mechanical part will be

$$m\frac{d^2x(t)}{dt^2} + \alpha\frac{dx(t)}{dt} + \beta\sin x(t) - Ki_a(t) = 0 \tag{6}$$

For the electrical subsystem, the following equivalent circuit model of the motor given in Fig. 3 can be used.

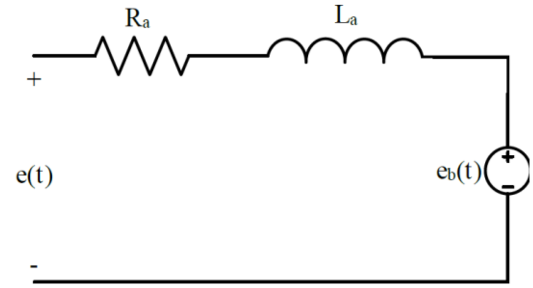

Fig. 3. Equivalent electrical circuit of a DC linear motor

Referring to Fig. 3, circuit equation will be

$$e(t) = R_a i_a + L_a\frac{di_a}{dt} + e_b(t) \tag{7}$$

where $e(t)$ is the applied voltage, which is also the control input to the system, R_a is the armature resistance, L_a is the armature inductance, and $e_b(t)$ is the back-emf voltage. Back-emf can simply be defined as

$$e_b(t) = Kv(t) \tag{8}$$

where $v(t)$ is the armature speed, which is equal to time-derivative of the position, $x(t)$. So the differential equation of the electrical subsystem can be written as

$$\frac{di_a}{dt} = -\frac{R_a}{L_a}i_a - \frac{K}{L_a}v(t) + \frac{1}{L_a}e(t) \tag{9}$$

Considering Eqs. (6) and (9) together, the state-space model of the motor can be obtained. Selecting state variables as

$$\begin{bmatrix} x_1(t) \\ x_2(t) \\ x_3(t) \end{bmatrix} = \begin{bmatrix} i_a(t) \\ v(t) \\ x(t) \end{bmatrix} \tag{10}$$

and taking their time-derivatives as

$$\begin{aligned} \dot{x}_1(t) &= -\frac{R_a}{L_a}i_a(\mathrm{t}) - \frac{K}{L_a}v(t) + \frac{1}{L_a}e(t) \\ \dot{x}_2(t) &= -\frac{\alpha}{m}v(t) - \frac{\beta}{m}\sin\big(x(t)\big) + \frac{K}{m}i_a(t) \\ \dot{x}_3(t) &= v(t) \end{aligned} \tag{11}$$

that yields

$$\begin{aligned} \dot{x}_1(t) &= -\frac{R_a}{L_a}x_1(\mathrm{t}) - \frac{K}{L_a}x_2(t) + \frac{1}{L_a}u(t) \\ \dot{x}_2(t) &= -\frac{\alpha}{m}x_2(t) - \frac{\beta}{m}\sin(x_3(t)) + \frac{K}{m}x_1(t) \\ \dot{x}_3(t) &= x_2(t) \end{aligned} \tag{12}$$

where $u(t) = e(t)$ is the control input signal, which is the applied voltage. State-space equations given in Eq. (12) gives the nonlinear system model and can also be used to define the control problem as in the following section. Note that the nonlinearity exhibited by the system given in Eq. (12) comes from the assumption of nonlinear load model. Instead of linearizing the system around the small neighborhood of an equilibrium point, a nonlinear controller will be designed.

https://doi.org/10.17758/URUAE27.UA0625149

III. CONTROL PROBLEM DEFINITION

By referring the dynamical model given in Eq. (12), control problem can be defined as follows; "Drive the motor position, $x_3(t)$, to a desired trajectory, $x_{3d}(t)$ by using the control input signal, $u(t)$". It is assumed that all the state variables are available for measurement and all the system parameters are known.

To quantify the performance of the controller to be designed, a position tracking error signal can be defined as follows.

$$e(t) = x_3(t) - x_{3d}(t) \tag{13}$$

Note that if it is proven $e(t) \to 0$ as $t \to \infty$, this necessarily means that $x_3(t) \to x_{3d}(t)$ as $t \to \infty$. Then the control objective will be accomplished. The following section shows the control design step-by-step for the problem defined above to prove $e(t) \to 0$ as $t \to \infty$.

IV. CONTROL DESIGN

It should be noted that the control objective is to stabilize the third state variable while the control input signal appears in the equation of the first state variable. In such cases, Backstepping Technique [13] offers a very useful tool to control designer. Investigating the error system dynamics given in Eq. (13) gives

$$\dot{e}(\mathrm{t}) = \dot{x}_3(\mathrm{t}) - \dot{x}_{3d}(t) \tag{14}$$

To apply the backstepping procedure, Substituting x_3 -dynamics from Eq. (12) and then adding and subtracting a virtual control input, x_{2d}, to the right-hand side of Eq. (14) yields

$$\dot{e}(\mathrm{t}) = x_2(\mathrm{t}) - \dot{x}_{3d}(\mathrm{t}) - x_{2d}(\mathrm{t}) + x_{2d}(t) \tag{15}$$

Defining the first backstepping variable as

$$h_1(t) \triangleq x_2(\mathrm{t}) - x_{2d}(t) \tag{16}$$

and designing the first virtual control input as

$$x_{2d}(t) \triangleq -k_e e(t) + \dot{x}_{3d}(t) \tag{17}$$

where $k_e$is a control gain, yields the final dynamics of the error signal as

$$\dot{e}(t) = -k_e e(t) + h_1(t) \tag{18}$$

Investigating h_1-dynamics yields

$$\dot{h}_1(t) = \dot{x}_2(\mathrm{t}) - \dot{x}_{2d}(t)$$

$$= -\frac{\alpha}{m}x_2(t) - \frac{\beta}{m}\sin x_3(t) + \frac{K}{m}x_1(t) - \frac{d}{dt}\{-k_e e(t) + h_1(t)\}$$
$$= -\frac{\alpha}{m}x_2(t) - \frac{\beta}{m}\sin x_3(t) + \frac{K}{m}x_1(t) + k_e[-k_e e(t) + h_1(t)] - \ddot{x}_{3d}(t)$$

At this point, adding and subtracting another virtual control input, $\frac{k}{m}x_{1d}(t)$ to the right hand side of h_1-dynamics and defining the second backstepping variable as

$$h_2(t) \triangleq x_1(t) - x_{1d}(t) \tag{19}$$

and designing the second virtual control input as

$$x_{1d}(t) = \frac{m}{K}\Big[-k_1 h_1(t) - e(t) + \frac{\alpha}{m}x_2(t) + \frac{\beta}{m}\sin x_3(t) + K_e^2 e(t) - k_e h_1(t) + \ddot{x}_{3d}(t)\Big] \tag{20}$$

where $k_1$is a positive control gain, yields

$$\dot{h}_1(t) = -k_1 h_1(t) - e + \frac{K}{m}h_2(t) \tag{21}$$

Investigating the h_2- dynamics given in Eq. (19) yields

$$\dot{h}_2(t) = \dot{x}_1(t) - \dot{x}_{1d}(t) \tag{22}$$

Substituting x_1-dynamics given in Eq. (12) and time derivative of x_{1d} given in Eq. (20) results in

$$h_2(t) = -\frac{R_a}{L_a}x_1(\mathrm{t}) - \frac{K}{L_a}x_2(t) + \frac{1}{L_a}u(t) + f(\cdot) \tag{23}$$

where $f(\cdot)$ is a function of the all measurable states and known parameters comes from the time derivative of x_{1d}. For the sakes of brevity and clarity, its explicit form is given in Appendix.
If the control input signal is designed as

$$u(t) = -k_2 h_2(t) - \frac{K}{m}h_1(t) - f(\cdot) + \frac{R_a}{L_a}x_1(\mathrm{t}) + \frac{K}{L_a}x_2(t) \tag{24}$$

where k_2 is a positive control gain, then the final dynamics for $h_2(t)$ will be

$$h_2(t) = -k_2 h_2(t) - \frac{K}{m}h_1(t) \tag{25}$$

The following theorem and its proof show the boundedness all signals in the closed loop system and prove whether the control objective given Section III is achieved.

Theorem: For the system given in Eq. (12), the control input signal given in Eq. (24) guarantees that all signal in the closed loop system are bounded and the control objective given in Section III is achieved.

Proof: Selecting the Lyapunov candidate as

$$V(t) = \frac{1}{2}e^2(t) + \frac{1}{2}h_1^2(t) + \frac{1}{2}h_2^2(t) \tag{26}$$

where its time derivative is

$$\dot{V}(t) = e(t)\dot{e}(\mathrm{t}) + h_1(t)\dot{h}_1(\mathrm{t}) + h_2(t)\dot{h}_2(t) \tag{27}$$

If the Eqs. (18), (21), and (25) are substituted into Eq. (27), it results in

$$\dot{V}(t) = -k_e e^2(\mathrm{t}) - k_1 h_1^2(\mathrm{t}) - k_2 h_2^2(t) \quad (28)$$

If the Eq. (26) and (28) are considered together, it leads to

$$V(t) = -\gamma V(t) \quad (29)$$

where γ is a positive constant. Eq. (29) means that

$$V(t) = V_0 exp\{-\gamma t\} \quad (30)$$

where V_0 is the initial condition of $V(t)$ and $exp\{\cdot\}$ is the natural logarithm function. Eq. (30) necessarily means that $V(t)$ goes to zero exponentially. So its components; $e(t)$, $h_1(t)$, and $h_2(t)$ also go to zero exponentially. This implies that all signals in the closed loop system are bounded and the control objective given in Section III is achieved.

V. Numerical Simulation

A numerical simulation of the controller given in the previous section has been done by using MATLAB/Simulink environment. Values of the system parameters have been determined by experimentally and given in Table I.

TABLE I: Values of the System Parameters

Parameter	Value
R_a	17.6 Ω
L_a	45 mH
K	200 N/A
M	15.88 kg
α	0.007 Nsec/m^2
β	2 N

The desired trajectory has been selected as a ramp function with an initial condition of 0.5, i.e.,

$$x_{3d}(t) = 0.5 + t \quad [\text{meter}] \quad (31)$$

which its time variation is seen in Fig. 4. During the simulations, all the initial conditions of the state variables are set to zero and the control gains are set to the values given in Table II.

TABLE II: Values of the Control Gains

Gain	Value
k_e	0.9
k_1	4.1
k_2	20.8

Fig. 5 shows the time-variation of the error signal. As it can be seen from the Fig. 5, position tracking error converges to zero exponentially. Fig. 6 shows the time-variation of the control input signal. As shown in Fig. 6, it is bounded and reasonable. Numerical simulation results given in Figs. 5&6 numerically prove the claim given in the Theorem in Section IV.

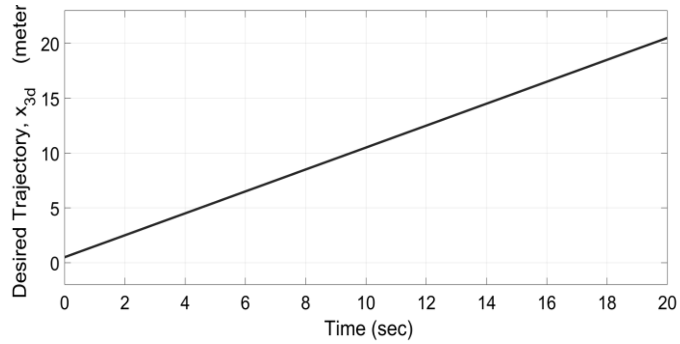

Fig. 4. Desired trajectory

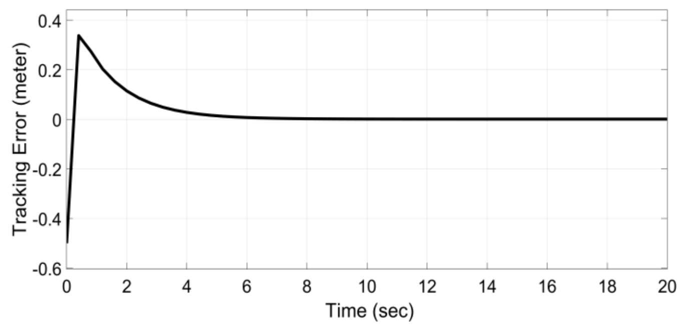

Fig. 5. Time variation of the tracking error

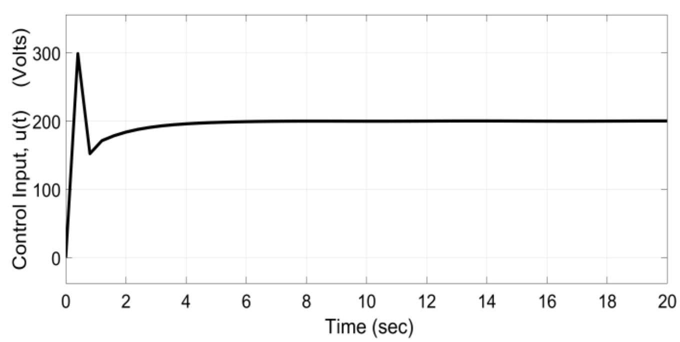

Fig. 6. Time variation of the control input signal

Sharp spikes at very beginning of the numerical simulation is due to the numerical derivation of the desired trajectory. For example, time-variations of the third numerical derivation of the desired trajectory is seen in Fig. 7., which such spikes are not expected in experimental operation.

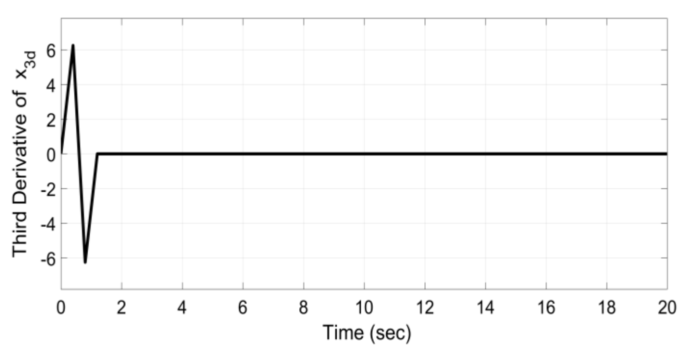

Fig. 7. Time-variation of the third numerical derivation of the desired trajectory

VI. Conclusion

A nonlinear speed controller for a novel permanent magnet DC linear motor has been presented. It has been shown that the controller is able to stabilize the system even in the existence of nonlinearities of the system dynamics. Numerical simulation results are in good agreement with the theoretical stability results. As shown by both theoretical analysis and simulation results, the speed tracking error converges to zero exponentially and all signals in the closed loop system are bounded.

The motor introduced in this study needs more control efforts. For example, the controller introduced in this study assumes all the system parameters are exactly known. But, on the other hand, another control scheme that assumes all the parameters are not exactly known could be more realistic and will be the future prospect.

Appendix

The explicit form of the function $f(\cdot)$ given in Eq. (23) is as follows.

$$
\begin{aligned}
f(\cdot) = \frac{m}{K}k_1\left[-k_1h_1(t) - e(t) + \frac{K}{m}h_2(t)\right] \\
&+ \frac{m}{K}\left[-k_e e(t) + h_1(t)\right] \\
&- \frac{\alpha}{K}\left[-\frac{\alpha}{m}x_2(t) - \frac{\beta}{m}sinx_3(t) + \frac{K}{m}x_1(t)\right] \\
&- \frac{\beta}{K}x_2(t)cosx_3(t) \\
&- \frac{m}{K}k_e^2\left[-k_e e(t) + h_1(t)\right] \\
&- \frac{m}{K}k_e\left[-k_1h_1(t) - e(t) + \frac{K}{m}h_2(t)\right] \\
&- \frac{m}{K}\dddot{x}_{3d}(t)
\end{aligned}
$$

Acknowledgment

The authors would like to thank to Prof. Recep Demirci for his valuable discussion. This work was supported in part by the Scientific and Technological Research Council of Turkiye (TUBITAK) under Grant 124E435.

References

[1] H. Yajima, H. Wakiwaka, S. Senoh, H. Yamada, and J. Oda, “Optimum design of a long stroke thin linear DC motor,” *Electrical Engineering in Japan*, vol. 118, no. 1, pp. 84–93, 1997.

[2] H. Yajima, H. Wakiwaka, K. Minegishi, N. Fujiwara, and K. Tamara, “Design of linear DC motor for high-speed positioning,” *Elsevier Sensors and Actuators*, vol.81, no. 1, pp. 281–284, 2000.

[3] R. C. Okonkwo, “Design and performance of permanent-magnet DC linear motors,” IEEE Transactions on Magnetics, vol. 42, no. 9, pp. 2179–2183, 2006.

[4] R. Demirci, and M. Dursun, “Adaptive position controller for double armature brushless dc linear motor,” *International Conference on Electrical Machines*, pp. 1-6, 2000.

[5] A. Basak, and A.F.F. Filho, “The design and analysis of a novel brushless DC linear motor,” *Journal of Magnetism and Magnetic Materials*, vol. 133, no. 3, pp. 640–643, 1994.

[6] J. Wang, W. Wang, and K. Atallah, “A linear permanent-magnet motor for active vehicle suspension,” IEEE Transactions on Vehicle Technologies, vol. 60, no. 1, pp. 55–63, 2011.

[7] A. Farhadi, H. Yousefi, Y. Norollahi, and A. Hajinezhad, “A comprehensive analysis on a novel DC-excited flux-switching linear motor as a new linear vehicle for transportation systems,” IET Electric Power Applications, vol 17, no. 1, pp. 36–46, 2023.

[8] Z. Demirkol. “Tubular DC Motor Design and Control,” Ph.D. dissertation, Dept. Elect. Eng., Duzce Univ., Duzce, Turkiye, 2023.

[9] Z. Demirkol, U. Hasirci, and R. Demirci, “Design, implementation and test of a novel cylindrical permanent magnet DC linear motor,” Energies, vol. 16, no. 8, pp. 1-17, 2023.

[10] Z. Demirkol, U. Hasirci, and R. Demirci, “A Linear Motor”, Turkish Patents, 2023.

[11] U. Hasirci, Z. Demirkol. Modeling and control of a novel permanent magnet linear motor. *Duzce University Journal of Science and Technology*, vol. 13, no. 1, pp. 346-356, 2025.

[12] The MathWorks, Inc. (2022). MATLAB version: 9.13.0 (R2022b). Accessed: January 01, 2023. Available: https://www.mathworks.com

[13] M. Krstic, I. Kanellakopoulos and P. V. Kokotovic, *Nonlinear and Adaptive Control Design*, 1st ed. Chichester, U.K.: Wiley, 1995, ch. 2, pp. 29-86.